Infrared Dielectric Dispersion and Apparent Ionic Charges in Sodium Nitrite

J. D. Axe
IBM, Watson Research Center, Yorktown Heights, New York
(Received 5 October 1967)

Measurements at room temperature of the infrared reflectivity of oriented samples of orthorhombic $NaNO_2$ crystals have been carried out and analyzed by Kramers-Kronig relations to obtain the principal dielectric response functions. The eight infrared dispersion frequencies found are well accounted for by the expected polar vibrational normal modes of the $NaNO_2$ lattice, as are the observed mode polarization directions. The range in magnitude of the dielectric polarization associated with the various normal modes is exceptionally large, and this feature has been further investigated by the use of a formalism in which apparent charges are assigned to the individual ions. The influence of dipolar local-field corrections on the apparent charges is considered within the context of a simplified "shell model," leading to a set of apparent ionic charges which explain the unusual intensity distribution within the modes in a natural way. The failure to observe resonant contributions to the dielectric response from phonons or other elementary excitations associated with the reorientation of the NO_2^- group and the attendant ferroelectric-paraelectric transition is discussed.

I. INTRODUCTION

At low temperatures, sodium nitrite ($NaNO_2$) exists in an ordered ferroelectric phase consisting of one formula unit per body-centered unit cell and belonging to the space group C_{2v}^{20} (see Fig. 1). At about 163°C, the spontaneous polarization disappears as a result of reorientations involving the sense of the NO_2^- group along the b axis.[1] Because both the structure and the structural nature of the spontaneous polarization appear to be relatively simple, $NaNO_2$ appears quite well suited for in-depth studies of various phenomena associated with order-disorder ferroelectrics.

Perhaps the most accessible and characteristic gauge of the state of a ferroelectrically orderable lattice is its dielectric response; thus studies of the low-frequency ($\leq 3\times 10^9$ Hz) dielectric dispersion and loss have been made on $NaNO_2$.[2–4] Largely in the hope of detecting certain elementary excitations predicted by a dynamical theory of the order-disorder transition, about which we shall have more to say later, we have extended these dielectric response studies to cover the infrared region by specular reflectance measurements.

Previous infrared studies of $NaNO_2$ have not been particularly concerned with the quantitative measurement of dielectric response as such, and furthermore, have concentrated on the high-frequency NO_2^- vibrations.[5–8] During the course of this work, however, Vogt and Happ[9] published the results of a study of the infrared reflectivity of $NaNO_2$ which they were able to combine with existing Raman-scattering data to propose normal vibrational mode assignments for the low-frequency modes. The inability to cover certain spectral ranges prevented a satisfactory discussion of the dielectric response, however.

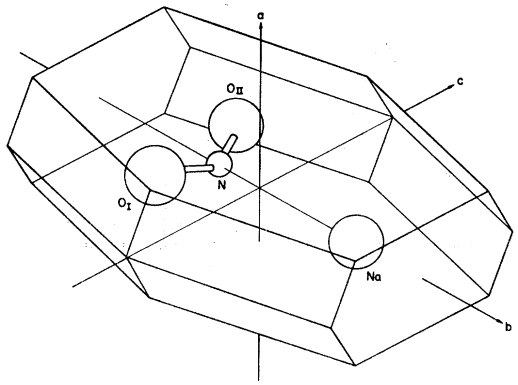

FIG. 1. The primitive body-centered orthorhombic unit cell of $NaNO_2$. The structural disorder at higher temperatures primarily results in equal numbers of NO_2^- groups with their apexes pointing in the $+b$ and $-b$ direction.

Section II presents the experimental results obtained by analysis of the spectral-reflectivity measurements. The resonant lattice contributions to the dispersion are analyzed in terms of normal vibrational modes, and the dipole strengths of these modes are found and commented upon. Section III contains a further discussion of the form of the normal modes, as well as a minimal development of a phenomenological treatment of lattice dispersion in order to introduce the concept of apparent ionic charges. This is followed by a calculation of the apparent ionic charges based upon a local dipole field treatment of a lattice of polarizable ions and provides a microscopic basis for the understanding of the observed mode dipole strengths. In Sec. IV the validity

[1] See F. Jona and G. Shirane, *Ferroelectric Crystals* (Pergamon Press, Inc., New York, 1963).
[2] S. Sawada, S. Nomura, and Y. Asao, J. Phys. Soc. Japan **16**, 2207 (1961).
[3] E. Nakamura, J. Phys. Soc. Japan **17**, 9611 (1962).
[4] I. Hatta, T. Sakudo, and S. Sawada, J. Phys. Soc. Japan **21**, 1612 (1966).
[5] R. Newman, J. Chem. Phys. **20**, 444 (1951).
[6] J. W. Sidman, J. Am. Chem. Soc. **79**, 2675 (1957).
[7] R. E. Weston, Jr., and T. F. Brodasky, J. Chem. Phys. **27**, 683 (1957).
[8] Y. Sato, K. Gesi, and Y. Takagi, J. Phys. Soc. Japan **16**, 2172 (1961).
[9] H. Vogt and H. Happ, Phys. Status Solidi **16**, 711 (1966).

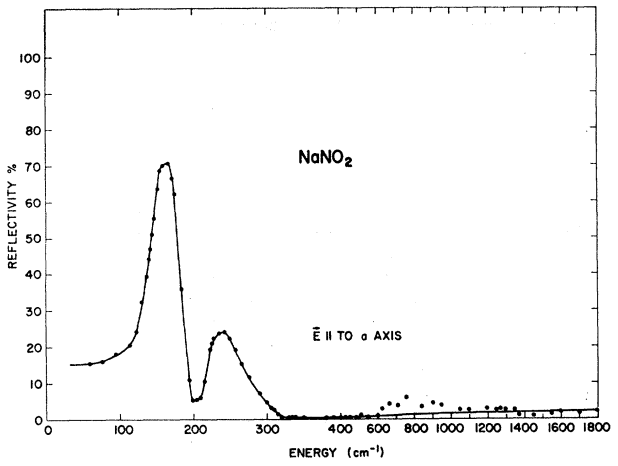

(a)

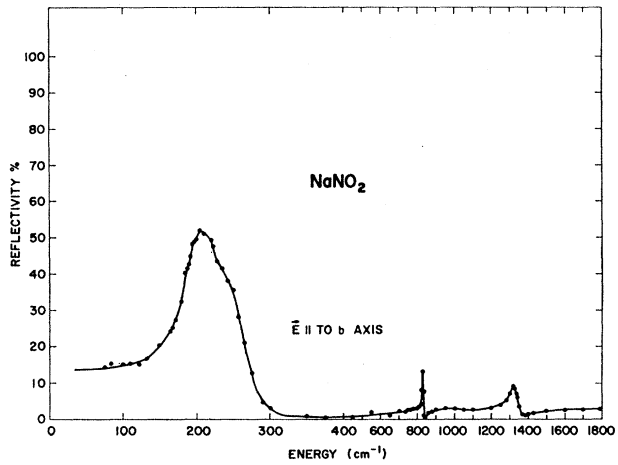

(b)

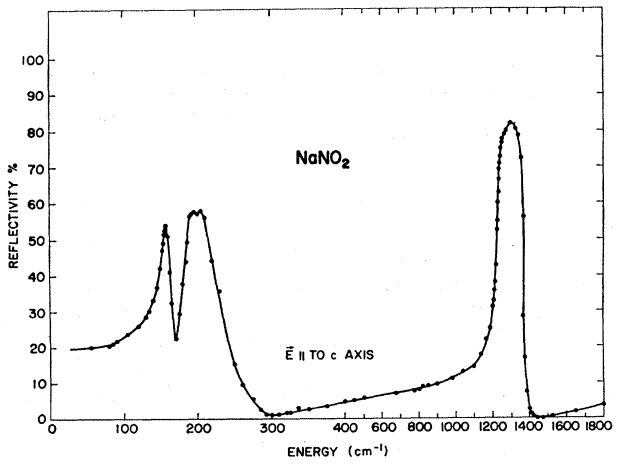

(c)

FIG. 2. The measured room-temperature spectral reflectivity of $NaNO_2$. The circles which represent data are connected by a smoothed curve. The three sets of data were taken with the electric vector of the radiation parallel to the *a*, *b*, and *c* axes of the crystal, respectively. Note the change of scale at 400 cm^{-1}.

of these results is discussed and the failure to observe the predicted excitations associated with the NO_2^- positional disordering is considered.

II. EXPERIMENTAL

$NaNO_2$ samples were prepared by slow cooling of the molten material in a polyethylene crucible from which single crystals with several cm^2 surfaces could readily be salvaged. Large flat (101) cleavage faces furnished excellent surfaces from which the reflectance for light polarized along the *b* axis was obtained. However, for the spectra polarized along the *a* and *c* axes, cut and polished (010) surfaces were used, and considerable difficulty was encountered in the preparation of these surfaces. Visually specular polishing could

TABLE I. Summary of parameters characterizing the infrared dispersion of $NaNO_2$.

	ω_{TO} (cm^{-1})	γ (cm^{-1})	$\Delta\epsilon'$	ω_{LO} (cm^{-1})
$E \parallel a$				
B_1(trans)	149	13±2	2.7±0.5	193
B_1(lib)	223	30±6	0.5±0.1	261
$\epsilon^\infty+\Sigma\Delta\epsilon'=5.1\pm0.6$[a]; $\epsilon^\circ_{meas}=5.2$[b]				
$\Pi(\omega_{LO}/\omega_{TO})^2=2.3$; $(\epsilon^\circ/\epsilon^\infty)_{meas}=2.86$				
$E \parallel b$				
A_1(trans)	194	27±5	2.3±0.3	269
A_1(NO_2 bend)	826	5±1	0.017±0.003	829
A_1(sym stretch)	1323	45±5	0.047±0.010	1336
$\epsilon^\infty+\Sigma\Delta\epsilon'=4.4\pm0.3$[a]; $\epsilon^\circ_{meas}=4.18$[b]				
$\Pi(\omega_{LO}/\omega_{TO})^2=1.9$; $(\epsilon^\circ/\epsilon^\infty)_{meas}=2.10$				
$E \parallel c$				
B_2(trans)	157	10±3	1.5±0.5	163
B_2(lib)	188	18±4	1.8±0.1	250
B_2(asym stretch)	1235	14±1	0.55±0.05	1368
$\epsilon^\infty+\Sigma\Delta\epsilon'=6.6\pm0.6$[a]; $\epsilon^\circ_{meas}=7.8$[b]				
$\Pi(\omega_{LO}/\omega_{TO})^2=2.4$; $(\epsilon^\circ/\epsilon^\infty)_{meas}=2.87$				

[a] Values of ϵ^∞ taken from Ref. 5.
[b] Measured at frequency of 3×10^9 Hz (Ref. 3).

readily be performed on heavy paper impregnated with a volatile organic solvent with or without fine alumina grit. However, such surfaces did not yield cleanly polarized spectra. Much cleaner polarization behavior was obtained by etching the polished crystals in a water-methanol mixture, but only at the expense of introducing some diffuse scattering, particularly at shorter wavelengths. In particular, the structure seen in the *a* polarization in the 600–800 cm^{-1} region and near 1200 cm^{-1} was very sensitive to surface treatment and is presumed spurious. Thus, although some effort was made to minimize reflectivity errors due to surface preparation, they remain the largest single source of uncertainty (±~5%) in some spectral regions. The reflectivities were measured at near-normal incidence using point-by-point comparison with an aluminized surface in a Perkin-Elmer 301 spectrometer. Pile-of-

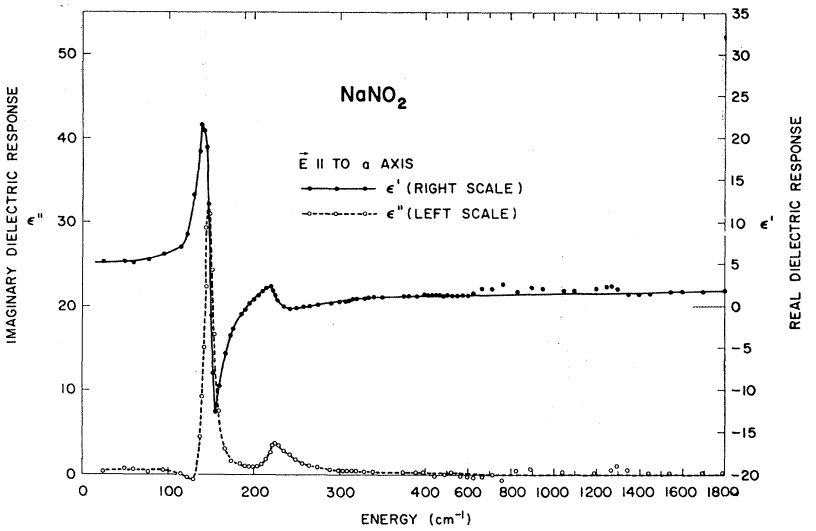

FIG. 3. The principal infrared dielectric response $\tilde{\epsilon}_{aa}=\epsilon_{aa}'+i\epsilon_{aa}''$. The circles represent values calculated from the measured reflectivity by Kramers-Kronig analysis and are connected by a smoothed curve. Note the change of scale at 400 cm^{-1}.

plates polarizers of both polyethylene and AgCl were used to cover the spectral range 50–4000 cm^{-1}. The room-temperature results are shown in Fig. 2. The principal dielectric response functions were derived from the measured reflectivities by numerical integration of the phase-shift dispersion relations[10] with the aid of an IBM 7094 digital computer. These results are shown in Figs. 3–5.

Neglecting small corrections due to finite damping, the frequencies of the long-wavelength transverse polar modes, $\omega_\alpha(\mathrm{TO})$, are given by the maxima in the imaginary dielectric response. The corresponding longitudinal frequencies, $\omega_\alpha(\mathrm{LO})$, are given by the alternative sets of frequencies for which $\epsilon(\omega)=0$.[11] The dipole strength of the αth transverse mode is conveniently characterized by its contribution to ϵ_{ii}^0, the static dielectric constant. This contribution, $\Delta\epsilon_{ii}^\alpha$, can be found by computing the contribution of the mode to the Kramers-Kronig integral

$$\epsilon_{ii}^0-\epsilon_{ii}^\infty=\frac{2}{\pi}\int\omega^{-1}\epsilon_{ii}''(\omega)\,d\omega.$$

The division of mode strength between incompletely resolved modes was estimated. These data, along with the widths of the ϵ'' resonances at half-maxima, γ_α, are tabulated in Table I.

Symmetry considerations establish that there are eight $\mathbf{q}=0$ optical normal modes of the ordered $NaNO_2$ lattice which are infrared active. (As is clear from Sec. III, there is a one-to-one correspondence between

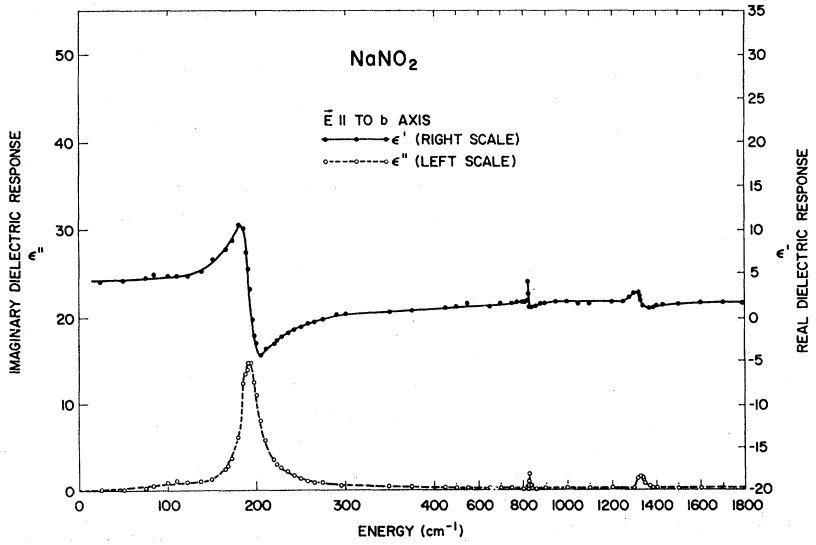

FIG. 4. The principal infrared dielectric response $\tilde{\epsilon}_{bb}$.

[10] F. Stern, in *Solid State Physics*, edited by F. Seitz and D. Turnbull (Academic Press Inc., New York, 1963), Vol. 15, p. 333.
[11] A. S. Barker, Phys. Rev. **136**, A1290 (1964).

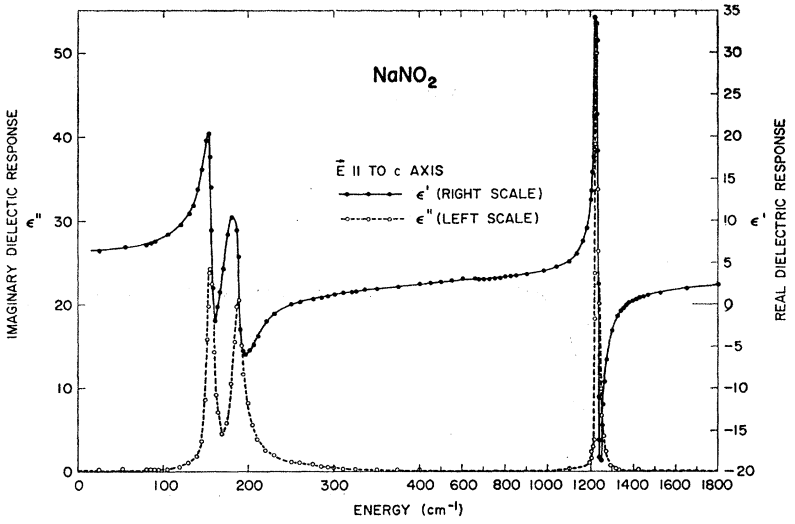

FIG. 5. The principal infrared dielectric response $\tilde{\epsilon}_{cc}$.

the number of such $\mathbf{q}=0$ modes and the number of transverse polar modes with a given small but nonvanishing $\mathbf{q}$ vector which give rise to dispersion, and it is simpler to do the group theory without worrying about the finite propagation vector.) These modes can be characterized by the irreducible representations of the point group C_{2v} according to which they transform, or equivalently, and more physically, simply by specifying the principal axis along which the dipole moment lies.[12] There are three A_1 modes (polarization parallel to b), three B_2 modes (polarization parallel to c), and two B_1 modes (polarization parallel to a). Two of the A_1 modes and one B_2 mode involve predominantly relative displacements within the nitrite group and might be expected to be at considerably higher frequencies than the remaining modes. There is one further optic mode of A_2 symmetry which is not infrared active and therefore not of present interest. Raman-scattering measurements place it at $\sim$122 cm^{-1}.[13,14]

The experimentally observed dispersion is in good agreement with the above normal-mode analysis, as is the predicted separation into low- and high-frequency modes. Our measurements at lower frequencies are generally in good agreement with those of Vogt and Happ, and there can be little doubt that their mode assignments, which are identical with ours, are correct. The internal NO_2^- modes have been previously identified[6,7] and the only serious discrepancy is seen to exist for the highest-frequency B_2 mode. As discussed in more detail by Tramer,[13] the wide variation of the observed frequencies and other rather anomalous behavior associated with this transition results from excitation of other than purely transverse modes in some sample geometries, e.g., powders. Such modes lie within a band of width $(\omega_{LO}-\omega_{TO})$, which is in this case large because of the unusually large dipole strength of the transition.[15] The present determination should be nearly free of such effects.

Having obtained the complete lattice dispersion, several more quantitative comparisons of the data can be made. Table I compares the sum of the optical plus infrared contributions to the static dielectric response with the measured low-frequency dielectric constant. The agreement is good in the a and b polarizations, showing that no important sources of dispersion exist between 50 cm^{-1} and the frequency of the microwave determination. (At still lower frequencies there is additional dispersion associated with the unclamping of the crystal and with the relaxation of the ferroelectric fluctuations.) The agreement is much poorer in the c direction, but we are inclined to dismiss the possibility of additional dispersion here as well, for as we have seen, all of the vibrational contributions are accounted for, and any "extra" contributions due to ferroelectric reorientations would be expected to appear predominantly in the b polarization.

Also, rather unsatisfactory is the accuracy with which the LO and TO mode frequencies in the a and c polarization satisfy the Lyddane-Sachs-Teller relation, which for orthorhombic crystals is

$$\epsilon_{ii}^0/\epsilon_{ii}^\infty=\prod[\omega_\alpha(\mathrm{LO})/\omega_\alpha(\mathrm{TO})]^2,$$

the product being restricted to modes polarized in the ith direction.[16] It is quite possible that the lack of agreement largely reflects errors due to surface preparation, the agreement in the b polarization is considerably better.

[12] We follow the convention of Ref. 9 in the choice of axes insofar as it affects the nomenclature of the irreducible representations.
[13] A. Tramer, Compt. Rend. **248**, 3546 (1959).
[14] E. V. Chisler and M. S. Shur, Phys. Status Solidi **117**, 163 (1966).
[15] J. D. Axe, Phys. Rev. **157**, 429 (1967).
[16] W. Cochran and R. A. Cowley, J. Phys. Chem. Solids **23**, 447 (1962).

Probably the most striking result of Table I is the unusual strength of the B_2 mode at 1235 cm^{-1}, some consequences of which have already been described. The quantum-mechanical transition probability associated with creating a phonon in this mode (proportional to $\Delta\epsilon_{ii}{}^{\alpha}\Omega_{\alpha}{}^2$) is some 10–60 times greater than for the remaining modes. In an effort to understand the reasons for such large differences in the mode dipole strength, in the following sections we apply to $NaNO_2$ a quantitative microscopic treatment of infrared dielectric dispersion. After defining, in a purely phenomenological manner the concept of an apparent ionic charge, we calculate the apparent charges for an $NaNO_2$ lattice composed of distinct electrically polarizable atomic ions and show that these considerations afford not only a natural explanation of the observed mode intensities, but indirectly some information on the form of the normal modes themselves.

III. APPARENT CHARGES IN A POLARIZABLE LATTICE

The concept of an apparent ionic charge derives naturally from a phenomenological discussion of dielectric dispersion in complex lattices first given by Born and Huang.[17] They show that the equations which describe the long-wavelength ($\mathbf{q}\to 0$) vibrations of a lattice can be written as

$$-m_k\ddot{u}_i(k)=\sum_{jk'}M_{ij}{}^{kk'}u_j(k')-\sum_j Q_{ji}{}^kE_j, \tag{1}$$

$$P_i=(1/v)\sum_{jk}Q_{ij}{}^ku_j(k)+\sum_j\chi_{ij}E_j, \tag{2}$$

$$\mathbf{E}=-4\pi(\mathbf{q}\cdot\mathbf{P}/|\,q\,|^2)\mathbf{q}+\mathbf{E}^0, \tag{3}$$

where $\mathbf{u}(k)\exp i(\mathbf{q}\cdot\mathbf{l})$ is the displacement of the kth ion in the $\mathbf{l}$th unit cell and $\mathbf{E}\exp i(\mathbf{q}\cdot\mathbf{l})$ and $\mathbf{P}\exp i(\mathbf{q}\cdot\mathbf{l})$ are, respectively, the macroscopic electric field and dielectric polarization. If there are n atoms in a unit cell, the dynamical matrix $\mathbf{M}$ is $3n\times 3n$, the apparent charge matrix $\mathbf{Q}$ is $3n\times 3$ and χ is by definition the 3×3 high-frequency susceptibility tensor. The meaning of the apparent charges is just $Q_{ij}{}^k=\partial P_i/\partial u_j(k)$. m_k is the mass of the kth ion. The electric field is the sum of the external field $\mathbf{E}^0\exp i(\mathbf{q}\cdot\mathbf{l})$ and that due to the polarization charge $-\mathrm{div}[\mathbf{P}\exp i(\mathbf{q}\cdot\mathbf{l})]$.

For a complex lattice it is often convenient to reexpress the displacements of the n bravais sublattices $\mathbf{u}(k)$ in terms of symmetry mode vectors $\mathbf{s}_{\alpha}{}^k$ which transform irreducibly under transformations which leave the lattice unchanged.

$$\mathbf{u}(k)=\sum_{\alpha}S_{\alpha}\mathbf{s}_{\alpha}{}^k. \tag{4}$$

S_{α}, the symmetry coordinate of the αth symmetry mode, contains the time dependence of $\mathbf{u}(k)$. The components of $\mathbf{s}_{\alpha}{}^k$ can be chosen to satisfy the orthogonality and completeness relations

$$\sum_{k,i}m_k s_{\alpha i}s_{\beta i}{}^k=M\delta_{\alpha\beta}, \tag{5}$$

and

$$\sum_{\alpha}m_k s_{\alpha i}{}^k s_{\alpha j}{}^{k'}=M\delta_{kk'}\delta_{ij}, \tag{6}$$

where $i,j=a,b,c$ and we choose to define the normalization constant $M=\sum_k m_k$.

Although $\mathbf{M}$, $\mathbf{Q}$, and χ are independent of $\mathbf{q}$, the eigensolutions of Eqs. (1)–(3) depend upon $\mathbf{q}$ through $\mathbf{E}(\mathbf{q})$ in Eq. (3), making solutions for general polarization and propagation directions complex. Fortunately, for lattices with orthorhombic or higher symmetry, the dielectric dispersion can be discussed by explicit consideration of only the modes with dipole moments along the three principal crystal axes and transverse to their propagation vector $\mathbf{q}$. The eigenfrequencies associated with such modes are known as dispersion frequencies. For such modes, $\mathbf{E}=0$ if there are no external fields; the modes are then simply eigensolutions of the dynamical matrix $\mathbf{M}$. We denote mode vectors which diagonalize $\mathbf{M}$ as normal mode vectors $\mathbf{n}_{\beta}{}^k$ and normalize them to obey Eqs. (5) and(6). The $\mathbf{n}_{\beta}{}^k$ of a given symmetry type are then related to the $\mathbf{s}_{\alpha}{}^k$ of the same symmetry type by a linear orthogonal transformation. In terms of the nonzero dispersion frequencies Ω_{β}, the dielectric response of the lattice can be written as[18]

$$\epsilon_{ij}(\omega)=\epsilon_{ij}{}^{\infty}+\sum_{\beta}\Delta\epsilon_{ij}{}^{\beta}\Omega_{\beta}{}^2/(\Omega_{\beta}{}^2-\omega^2), \tag{7}$$

$$\Delta\epsilon_{ij}{}^{\beta}=(4\pi X_i{}^{\beta}X_j{}^{\beta}/M\Omega_{\beta}{}^2v), \tag{8}$$

$$\epsilon_{ij}{}^{\infty}=1+4\pi\chi_{ij}, \tag{9}$$

where we have defined a dispersion mode charge vector $\mathbf{X}^{\beta}$ given by

$$X_i{}^{\beta}=\sum_{kj}Q_{ij}{}^k\mathbf{n}_{\beta j}{}^k. \tag{10}$$

Physically, $\mathbf{X}^{\beta}$ is seen to be directly proportional to the dipole moment associated with the βth normal mode. Although $\mathbf{X}^{\beta}$ is in general a vector, it is clear by inspection of Eq. (8) that for crystals with orthorhombic and higher symmetry, a given mode vector has but a single component along one or another of the principal axes. We will subsequently treat $\mathbf{X}^{\beta}$ as a scalar.

[17] M. Born and K. Huang, *Dynamical Theory of Crystal Lattices* (Oxford University Press, New York, 1964). Equations (13)–(18) can also be formally obtained from a more general so-called "shell" model by allowing the shell charges Y_k and the shell core coupling constants K_k to increase without limit in such a way that the net ion charges Z_k and polarizabilities $Y_k{}^2/K_k$ remain finite. Physically, these assumptions have the effect of suppressing polarization effects due to nonelectrostatic short-range forces. See Ref. 25 for a further discussion.

[18] The development of symmetry mode coordinates is, with a change of notation, that of D. A. Kleinman and W. G. Spitzer, Phys. Rev. **125**, 16 (1961).

TABLE II. Polar symmetry mode vectors $s_\alpha{}^k$ for $NaNO_2$. The results, normalized according to Eq. (5), are tabulated as row vectors with components along the a, b, c crystal axes.

	Na			N			O_I			O_{II}		
	a	b	c	a	b	c	a	b	c	a	b	c
A_1(sym stretch)	...	...	...	...	−1.629	...	...	0.712	0.696	...	0.712	−0.696
A_1(bend)	...	...	...	...	−0.879	...	...	0.384	−1.295	...	0.384	1.295
A_1(trans)	...	1.414	...	...	0.707	...	...	0.707	...	...	0.707	...
B_1(lib)	...	...	...	1.853	...	...	0.810	...	...	0.810	...	...
B_1(trans)	1.414	...	...	0.707	...	...	0.707	...	...	0.707	...	...
B_2(asym stretch)	...	...	...	...	...	1.745	...	−0.487	−0.763	...	0.487	−0.763
B_2(lib)	...	...	...	...	...	0.616	...	1.387	−0.269	...	−1.387	−0.269
B_2(trans)	...	...	−1.414	...	...	0.707	...	...	0.707	...	...	0.707

The apparent charge tensors must be invariant to all the symmetry operations of the unit cell, which in the case of $NaNO_2$ restricts the form to

$$\mathbf{Q}^{(\mathrm{Na})}=\begin{pmatrix} Q_{aa}{}^{(\mathrm{Na})} & 0 & 0 \\ 0 & Q_{bb}{}^{(\mathrm{Na})} & 0 \\ 0 & 0 & Q_{cc}{}^{(\mathrm{Na})} \end{pmatrix}$$

$$\mathbf{Q}^{(\mathrm{N})}=\begin{pmatrix} Q_{aa}{}^{(\mathrm{N})} & 0 & 0 \\ 0 & Q_{bb}{}^{(\mathrm{N})} & 0 \\ 0 & 0 & Q_{cc}{}^{(\mathrm{N})} \end{pmatrix}$$

$$\mathbf{Q}^{(\mathrm{O_I})}=\begin{pmatrix} Q_{aa}{}^{(\mathrm{O})} & 0 & 0 \\ 0 & Q_{bb}{}^{(\mathrm{O})} & Q_{bc}{}^{(\mathrm{O})} \\ 0 & Q_{cb}{}^{(\mathrm{O})} & Q_{cc}{}^{(\mathrm{O})} \end{pmatrix}$$

$$\mathbf{Q}^{(\mathrm{O_{II}})}=\begin{pmatrix} Q_{aa}{}^{(\mathrm{O})} & 0 & 0 \\ 0 & Q_{bb}{}^{(\mathrm{O})} & -Q_{bc}{}^{(\mathrm{O})} \\ 0 & -Q_{cb}{}^{(\mathrm{O})} & Q_{cc}{}^{(\mathrm{O})} \end{pmatrix}. \quad (11)$$

Note that $\mathbf{Q}^k$ is not in general symmetric. Translational invariance imposes the additional restraint $\sum_k Q_{ij}{}^k=0$. There are thus eight independent apparent charge parameters necessary to describe the lattice dispersion in $NaNO_2$.

Since the high-frequency A_1 and B_2 modes are largely "internal" NO_2^- vibrations, the dynamical matrix can be approximately factored into high- and low-frequency parts by choosing "external" symmetry vectors involving translations and rotations of the rigid NO_2^- group and internal symmetry vectors orthogonal to them. Insofar as the internal NO_2^- vibrations are concerned, it is possible to be even more restrictive. Weston and Brodasky[7] have measured the internal vibrational frequencies of $N^{14}O_2^-$ and $N^{15}O_2^-$ in a variety of diluents. From these data they were able to determine the constants in a general valence potential function,

$$2V=f_d(\Delta d_1{}^2+\Delta d_2{}^2)+2f_{dd}\Delta d_1\Delta d_2+f_2\Delta\alpha^2 +2f_{dd}(\Delta d_1+\Delta d_2)\Delta\alpha, \quad (12)$$

where Δd_1 and Δd_2 are changes in the N–O bond lengths and $\Delta\alpha$ is a change in the O–N–O bond angle. They find this truncated potential to be reasonably adequate, as one might infer from the observation that the internal vibrational frequencies differ by a few percent at most in widely different environments.[6,7] We can take advantage of the fact that the NO_2^- vibrations are largely internally determined by choosing the internal symmetry coordinates which diagonalize the valence potential function. This particular choice of internal symmetry coordinates should be a good approximation to the true internal normal modes and we shall treat them as such. Of the remaining symmetry mode vectors involving Na^+ displacements and rigid NO_2^- translations and librations, two, A_1(trans) and A_2(lib), are uniquely determined by symmetry considerations and the requirement that they be orthogonal to the internal NO_2^- mode vectors, and are thus approximate normal modes as well. (In fact, the form of the A_2 mode is precisely determined by symmetry considerations alone, but because it has no dipole moment it is not of present interest.) It is only for the two low-frequency B_1 modes and B_2 modes that the choice of symmetry mode vectors remains arbitrary. For the present we make the simplest choice consisting of a pure NO_2^- libration and a pure Na^+–NO_2^- translatory motion. We will later have an opportunity to examine how physical this choice is, i.e., how closely these idealized motions approximate normal modes. The symmetry mode vectors are given in Table II.

The apparent ionic charges are useful in "understanding" the over-all infrared dispersion of a system. In general, however, they are not unambiguously defined by dispersion measurements alone. This forces us to examine the factors determining the $\mathbf{Q}^k$ in greater detail, and to attempt to estimate them on the basis of a rather simple model.

TABLE III. Lorentz factor matrices between bravais sublattices in $NaNO_2$. $\gamma^{k,k'}=\gamma^{k',k}$.

$$\gamma^{\mathrm{Na,Na}}=\gamma^{\mathrm{N,N}}=\gamma^{\mathrm{OI,OI}}=\gamma^{\mathrm{OII,OII}}=\begin{matrix}\\ i'\\ j'\\ k'\end{matrix}\begin{matrix}\begin{matrix}i & j & k\end{matrix}\\ \begin{pmatrix}6.041 & 0 & 0\\ 0 & 3.314 & 0\\ 0 & 0 & 3.212\end{pmatrix}\end{matrix}$$

$$\gamma^{\mathrm{Na,N}}=\begin{pmatrix}0.069 & 0 & 0\\ 0 & 8.369 & 0\\ 0 & 0 & 4.128\end{pmatrix}\qquad \gamma^{\mathrm{Na,OI}}=\begin{pmatrix}4.095 & 0 & 0\\ 0 & 3.782 & -4.795\\ 0 & -4.795 & 4.689\end{pmatrix}$$

$$\gamma^{\mathrm{Na,OII}}=\begin{pmatrix}4.095 & 0 & 0\\ 0 & 3.782 & 4.795\\ 0 & 4.795 & 4.689\end{pmatrix}\qquad \gamma^{\mathrm{N,OI}}=\begin{pmatrix}-22.719 & 0 & 0\\ 0 & 0.628 & 39.508\\ 0 & 39.508 & 34.656\end{pmatrix}$$

$$\gamma^{\mathrm{N,OII}}=\begin{pmatrix}-22.719 & 0 & 0\\ 0 & 0.628 & -39.508\\ 0 & -39.508 & 34.656\end{pmatrix}\qquad \gamma^{\mathrm{OI,OII}}=\begin{pmatrix}12.148 & 0 & 0\\ 0 & 0.862 & 0\\ 0 & 0 & 13.852\end{pmatrix}$$

Suppose that the electrons in an insulating solid could be apportioned to the individual nuclei in some meaningful way so that each ion has some net static charge Z_k. Then, if the nuclei carried their charge distributions rigidly with them during displacement, the effective-charge tensor would be diagonal with $Q_{ii}{}^k=Z_k$. In reality, the periodic dipole array set up by a given sublattice displacement produces local electric fields[19] at the sites of all the sublattices, and because the ions are themselves electrically polarizable, this gives rise to additional polarization. This effect makes an important contribution to the apparent charges of polarizable ions, and is rather simply calculated in the local dipole field approximation, in which it is assumed that each ion makes an electronic contribution to the dipole moment (in addition to that caused by nuclear displacements) just proportional to the local electric field at the ion site. Born and Huang[17] have derived expressions for the high-frequency susceptibility and the apparent charge tensor of a lattice in this approximation, and they can be written as follows:

$$\chi_{ij}{}^{\infty}=(\epsilon_{ij}{}^{\infty}-1)/4\pi=(1/v)\sum_{k,k'}\Gamma_{ij}{}^{kk'}, \tag{13}$$

$$Q_{ij}{}^{k}=Z_k[1-\sum_{k'}(C\Gamma)_{ij}{}^{kk'}], \tag{14}$$

where $\mathbf{C}$ and $\mathbf{\Gamma}$ are closely related to the Lorentz factor matrix $\boldsymbol{\gamma}$ relating $\mathbf{F}^k$, the local field at sublattice k, with $\mathbf{P}^{k'}$, the dielectric polarization at sublattice k', i.e.,

$$F_i{}^k=E_i{}^k+\sum_{jk'}\gamma_{ij}{}^{kk'}P_j{}^{k'}. \tag{15}$$

In terms of $\boldsymbol{\gamma}$ and a polarizability matrix $\alpha_{ij}{}^{kk'}=\alpha_{ij}{}^k\delta_{kk'}$, where $\boldsymbol{\alpha}^k$ is the electronic polarizability tensor of the kth ion, $\mathbf{\Gamma}$ is defined by

$$(\Gamma^{-1})_{ij}{}^{kk'}=[(\alpha^{-1})_{ij}{}^{kk'}-(1/v)\gamma_{ij}{}^{kk'}] \tag{16}$$

and

$$C_{ij}{}^{kk'}=-(1/v)\gamma_{ij}{}^{kk'}\qquad \text{for } k=k', \tag{17}$$

and

$$Z_kC_{ij}{}^{kk}=-\sum_{k'\neq k}Z_{k'}C_{ij}{}^{kk'}, \tag{18}$$

v being the volume of the unit cell. For diagonally cubic crystals (each ion having tetrahedral or higher symmetry), Eq. (12) gives the familar Lorenz-Lorentz result, $\chi_{ij}{}^{\infty}=\delta_{ij}(\sum_k\alpha_{ii}{}^k/v)/(1-4\pi\sum_k\alpha_{ii}{}^k/3v)$, and Eq. (13) reduces to $Q_{ij}{}^k=\frac{1}{3}[\delta_{ij}Z_k(\epsilon_{ii}{}^{\infty}+2)]$.

The work of Szigeti[20] has demonstrated that the simple considerations of the previous paragraph are capable of nearly quantitative understanding of dispersion in simple ionic lattices, there being a residual 10–30% discrepancy associated largely with polarization effects arising from short-range forces. We shall proceed to apply this formulation to $NaNO_2$, and postpone discussion of the obvious conceptual difficulties associated with ionic charges and polarizabilities in materials with mixed ionic and covalent bonding.

The dipole sums occurring in the calculation of the Lorentz-factor matrix $\boldsymbol{\gamma}$ were performed with the aid of an IBM 7090 digital computer using the planewise summation method of DeWette and Schacher,[21] and published structural data.[22] The results given in Table III depart greatly from the well-known cubic result, $\gamma_{ij}{}^{kk'}=-\frac{4}{3}\pi\delta_{ij}$. The next step involved the assignment of electronic polarizabilities to the individual ions so as

[19] These local fields vary rapidly within a unit cell as opposed to the long-wavelength macroscopic field.

[20] B. Szigeti, Proc. Roy. Soc. (London) **A204**, 51 (1960).

[21] F. W. DeWette and G. E. Schacher, Phys. Rev. **137**, A78 (1965).

[22] M. I. Kay and B. C. Frazer, Acta Cryst. **14**, 56 (1961).

TABLE IV. Apparent ionic charges for $NaNO_2$. All charges are in units of $|e| = +4.8\times10^{-10}$ esu.

$Z_{Na}=1$	$Z_N=0.5$	$Z_O=-0.75$
$Q_{aa}^{Na}=1.32$	$Q_{bb}^{Na}=1.26$	$Q_{cc}^{Na}=1.58$
$Q_{aa}^{N}=-0.22$	$Q_{bb}^{N}=0.52$	$Q_{cc}^{N}=2.32$
$Q_{aa}^{O}=-0.55$	$Q_{bb}^{O}=-0.89$	$Q_{cc}^{O}=-1.95$
	$Q_{bc}^{O}=-0.44$ $Q_{cb}^{O}=-0.76$	

to give reasonable agreement with the observed high-frequency dielectric response through Eq. (12). In so doing, the following assumptions were made:

(1) All polarizabilities were taken to be isotropic, $\alpha_{ij}{}^k=\alpha^k\delta_{ij}$.

(2) For Na the Tessman-Kahn-Shockley value, $\alpha^{Na}=0.40$ Å^3 was used.

(3) Because a high formal charge and consequent low polarizability were anticipated for the nitrogen by comparison with the oxygens, α^N was set equal to zero. This leaves a single adjustable parameter α^O, with which to fit the three components of $\boldsymbol{\varepsilon}^\infty$. The fitting was done by trial and error, and it was found that over a small range of values of α^O rather good agreement was possible. For subsequent calculations $\alpha^O=1.45$ Å^3 was chosen, giving $\epsilon_{aa}{}^\infty=\epsilon_{bb}{}^\infty=1.92$ and $\epsilon_{cc}{}^\infty=2.49$, to be compared with the measured[5] values $\epsilon_{aa}{}^\infty=1.82$, $\epsilon_{bb}{}^\infty=1.99$, and $\epsilon_{cc}{}^\infty=2.62$.

Having arrived at a set of polarizabilities, it is only necessary to specify a set of static charges Z_k in order to calculate the apparent charge matrices through Eq. (13). Here we accepted $Z_{Na}=+|e|$ as sacrosanct, so that the remaining static charges could be written $Z_N=(3-2\delta)|e|$ and $Z_O=-(2-\delta)|e|$. The apparent charge tensors were then calculated as a function of δ, and upon combining the $\mathbf{Q}(\delta)$ so calculated with the symmetry mode vectors $\mathbf{s}_\alpha{}^k$ of Table II according to Eq. (10), a set of symmetry mode charges $\mathbf{X}^\beta(\delta)$ were obtained. But according to the previous discussion, four of the eight symmetry modes should be reasonable approximations to the true normal modes, and the calculated symmetry mode charges for these modes can thus be meaningfully compared with the actual $\mathbf{X}^\beta$ determined from the measured values of $\Delta\epsilon^\beta$ and Ω^β by Eq. (8). The result of this comparison is that only for values of δ near 1.25 is reasonable agreement possible. Table IV gives the resulting apparent ion charges and a comparison of the resulting calculated mode charges with the corresponding experimental quantities. Additional comparisons were obtained from a useful sum rule,

$$\sum_\beta |X_i{}^\beta|^2=\sum_{kj}(M/m_k)|Q_{ij}{}^k|^2, \qquad (19)$$

which follows immediately from the definition of $\mathbf{X}^\beta$ and the completeness relation between the normal mode vectors $\mathbf{n}_\alpha{}^k$, Eq. (6).

There are several points in Table IV worthy of note. First of all, it appears from a comparison of the apparent charge components $Q_{ij}{}^k$ with the assumed static charges Z_k that the polarization effects which we are calculating are far from negligible. Secondly, the large B_2(stretch) dipole strength, mentioned previously and revealed in Table V by the large observed mode charge, is well approximated by the use of the $\mathbf{Q}^k$ of Table V. To state the underlying cause as nearly perfect constructive superposition of individual atomic moments would seem to be correct but deceptively simplified. Since in all of the inner NO_2^- vibrations the nitrogen and oxygen atoms are moving out of phase (the motions must be orthogonal to the uniform NO_2 translation), we might expect roughly constructive superposition of dipoles and thus high mode strengths for all of these modes. If, for example, we use the assumed Z_k in place of the Q_k to calculate the mode charges, we find $X[A_1(\text{stretch})]=2.02|e|$, $X[A_1(\text{bend})]=1.02|e|$, and $X[B_2(\text{stretch})]=1.89|e|$. The point to be made is that the large value of $X[B_2(\text{stretch})]$ relative to the other two internal mode charges depends critically upon having nonisotropic and/or nondiagonal apparent charges. Furthermore, the local dipole field model seems capable of introducing these features in about the correct proportions.

The ability of the calculated $\mathbf{Q}^k$ to predict the sum $\sum_\beta |X_i{}^\beta|^2$ inspires confidence in the method at least as much as does the good agreement for the individual mode charges. Because it seems improbable that the sum rule would work so well if the $\mathbf{Q}^k$ were grossly in error, it appears that the lack of agreement between the measured mode charges and the mode charges calculated for the idealized B_1 and B_2 symmetry modes of low frequency must be ascribed to an incorrect description of the mode eigenvectors rather than to shortcomings of the apparent ionic charges. It is therefore quite likely that the low-frequency B_1 and B_2 modes can be approximately described only as complex inter-

TABLE V. Comparison of calculated symmetry mode charges and observed normal mode charges.

Symmetry mode	$\lvert X\rvert_{calc}$	$\lvert X\rvert_{obs}$	Normal mode freq (cm^{-1})
A_1(stretch)	2.73	2.49±0.25	1323
A_1(bend)	0.00	0.94±0.06	826
A_1(trans)	2.68	2.58±0.17	194
B_1(stretch)	7.76	7.96±0.36	1235
B_2(lib)	0.38	2.20±0.06	188
B_2(trans)	3.34	1.68±0.28	157
B_1(lib)	0.49	1.41±0.13	223
B_1(trans)	2.80	2.14±0.20	149
	calc	obs	
$\sum_{A1\text{ modes}}\lvert X^\beta\rvert^2$	14.64	13.7±1.3	
$\sum_{B1\text{ modes}}\lvert X^\beta\rvert^2$	8.08	6.6±1.2	
$\sum_{B2\text{ modes}}\lvert X^\beta\rvert^2$	71.6	71.0±8.0	

mixtures of the appropriate translational and librational motions.

IV. DISCUSSION

From a pragmatic viewpoint, the results Sec. III seem to justify the discussion of the high-frequency susceptibility and the apparent charges within the context of the local dipole field model. But is the model physically sensible? The problem, of course, is that as the bonding becomes less and less ionic the meaning of assigning individual charges and polarizabilities to the atoms becomes less and less clear. What we are really considering is a case with mixed bonding, i.e., the bonding between the Na ion and the entire NO_2 group should be ionic enough to justify separation of a Na ion charge and polarizability. Fortunately, it is possible to discuss just this portion of the calculation as well. This is so because the quantity $\mathbf{Q}^{\mathrm{Na}}/Z_{\mathrm{Na}}$ turns out to be nearly independent of δ, that is to say, we calculate that $Q_{aa}{}^{\mathrm{Na}} \approx Q_{bb}{}^{\mathrm{Na}} \approx 1.3 \mid e \mid$ and $Q_{cc}{}^{\mathrm{Na}} \approx 1.6 \mid e \mid$ irrespective of how the net negative charge is distributed over the NO_2^-. Fortunately again, the low-frequency A_1 mode is especially simple with a mode charge directly proportional to $Q_{bb}{}^{\mathrm{Na}}$, so that a direct comparison is possible. There can be little doubt that the good agreement obtained here is meaningful. Of course, as a result of translational invariance the net apparent charge tensor for the NO_2^- group as a whole is $\mathbf{Q}^{(\mathrm{NO_2})} = -\mathbf{Q}^{\mathrm{Na}}$.

This is probably an appropriate place to make clear the distinction between the *apparent* charge tensors $\mathbf{Q}^k$ and the scalar *effective* charges Z_k', introduced by Szigeti.[20] The $\mathbf{Q}^k$ are simply the first terms in a series expansion of $\partial P/\partial u(k)$ and provide a phenomenological description of lattice polarization. Szigeti's effective charges Z_k' are at the next higher level of abstraction. They are the values which the static charges Z_k need assume so that when modified or "dressed" by dipole local field effects they produce the correct $\mathbf{Q}^k$. Szigeti[20] has discussed the significance of effective charges and their deviation from formal charges in ionic compounds. The closed expressions for Z' he has given for cubic diatomic lattices can easily be obtained as a special case from the equations of Sec. III. The Szigeti effective charges $Z'_{\mathrm{Na}} = -Z'_{\mathrm{NO_2}}$ can be obtained from the data in Table V by changing Z_{Na} slightly until the measured and calculated values of $X[A_1(\mathrm{trans})]$ are in perfect agreement. We find in this way $Z'_{\mathrm{Na}} = 0.96(\pm 0.06) \mid e \mid$. The small deviation of Z'_{Na} from $1\times \mid e \mid$ can be taken as a quantitative measure of the relative unimportance of the combined effects of short-range polarization and covalency between the Na^+ and the NO_2^- ions.

If the orbital electronic states of the NO_2^- ion are approximated by functions of the form $\Psi = N(\psi_{\mathrm{N}} + \lambda\psi_{\mathrm{O}})$, where ψ_{N} and ψ_{O} represent separately normalized linear combinations of atomic orbitals centered at the nitrogen and oxygen nuclei, there is no unique way of assigning the charge if ψ_{N} and ψ_{O} overlap. In simplest approximate terms the charge distribution within the NO_2^- group can be described by assigning the fraction $1/(1+\lambda^2)$ of the charge of each electron in the orbital to the nitrogen, the remainder to the oxygens. McEwen[23] has determined a set of such molecular orbitals (linear combinations of atomic orbitals) for NO_2^- which give a good representation of the low-energy electronic spectrum. The values of Z_{N} and Z_{O} deduced from these molecular orbitals are in very good agreement with the values required in Sec. III, so that this latter set must at least be considered highly reasonable in the light of present knowledge.

The significance of separate polarizabilities α_{N} and α_{O} is even more difficult to discuss satisfactorily from a fundamental point of view, and falls beyond the scope of this paper. Empirically, however, it may be pointed out that some success has been achieved in correlating the optical refractivity of a large number of carbonate minerals in terms of individual atomic polarizabilities.[24] In fact, the range of values of α_{O} necessary to explain the carbonate refraction (1.3–1.4 Å^3) is very similar to the value $\alpha_{\mathrm{O}} = 1.45$ Å^3 needed for $NaNO_2$ (and considerably less than the Tessman-Kahn-Shockley value of 2.4 Å^3 deduced for more ionic compounds). Undoubtedly the present agreement between the observed and calculated optical dielectric response could be further improved by introduction of a nonzero $\boldsymbol{\alpha}_{\mathrm{N}}$, by a nonisotropic $\boldsymbol{\alpha}_{\mathrm{N}}$, or both. However, it is our belief that any such elaborations could be more satisfactorily made when the theoretical foundations for such refinements are better understood.

In $BaTiO_3$ and related materials, the dynamics of the ferroelectric transition are intimately connected with displacements consisting of phonon modes against which, essentially, the lattice becomes unstable.[25] In contrast to ferroelectrics of this type, which have been termed displacive, are materials of the present type which even in the paraelectric state have two or more possible configurations of a unit cell differing by finite reorientations or displacements. Each unit cell has a permanent dipole moment, but above a critical temperature there is a loss of long-range ordering of the dipoles and a resultant loss of the net spontaneous polarization. By analogy with the unstable phonon modes in displacive ferroelectrics, one might try to describe the dynamics of such an order-disorder transition in terms of elementary excitations of the lattice, and there have been several recent discussions from this point of view.[26–28] It is found that the essential

---

[23] K. L. McEwen, J. Chem. Phys. **34**, 547 (1961). Miss McEwen's calculation is explicit for the four π-bonding and six σ-nonbonding electrons. Following her suggestion, we consider the four σ-bonding electrons to be nonpolar ($\lambda = 1$), and the remaining $[(1S)_{\mathrm{N}}{}^2, (1S)_{\mathrm{O}}{}^2(2S)_{\mathrm{O}}{}^2]$ electrons to be fully localized. In this way we calculate $Z_{\mathrm{N}} = 0.49 \mid e \mid$, $2Z_{\mathrm{O}} = -1.49 \mid e \mid$.

[24] W. N. Lawless and R. C. DeVries, J. Phys. Chem. Solids **25**, 1119 (1964).

[25] W. Cochran, Advan. Phys. **9**, 387 (1960); R. A. Cowley, Phys. Rev. **134**, A981 (1964).

[26] P. G. De Gennes, Solid State Commun. **1**, 132 (1963).

[27] R. Brout, K. Müller, and H. Thomas, Solid State Commun. **4**, 507 (1966).

[28] J. Villain and S. Stamenkovic, Phys. Status Solidi **15**, 585 (1966).

features of an order-disorder transition can be incorporated into a Hamiltonian similar to those encountered for magnetically ordered lattices, giving rise to new elementary excitations analogous to magnetic spin waves, representing the finite displacements between alternate configurations. Furthermore, these treatments predict that the ferroelectric ordering and the associated anomalous dielectric susceptibility are direct consequences of the frequency of this "spin-wave"-like mode tending to zero near the characteristic ordering temperature. These are modes of excitation which exist in addition to the phonon excitations representing infinitesimal displacements about the equilibrium configurations. Experimental evidence for such extra "soft" modes in order-disorder ferroelectrics is less than conclusive.[29,30] The interpretation of infrared and neutron-scattering experiments on the most extensively studied materials such as the hydrogen phosphates and triglycine sulfate are made difficult because of the complexity of the lattices. Because $NaNO_2$ is perhaps the structurally simplest known order-disorder ferroelectric, the present study was partially undertaken to search for direct evidence for "extra" modes associated with the positional disordering, as we mentioned in the Introduction.

Several independent kinds of measurements have established that $NaNO_2$ is nearly completely ordered at room temperature. Simple theory predicts that the spin-wave-like mode frequency in the ordered lattice should be of order kT_c/h, well within the range of the present measurements.

Our results give no direct evidence for such a mode, and in fact show with some certainty that the gross features of the infrared dispersion arises from normal phonon excitations. One factor possibly involved in the failure to observe the predicted mode is that it may be heavily damped. The additional dispersion in ϵ_{bb} below 3×10^9 Hz shows a Debye relaxation behavior which would be consistent with the spin-wave formulation only if the mode were overdamped. In addition to the preceding argument, we can speculate that the quantum transitions associated with the excitations may be weak as well. It is not difficult to show that at temperatures well below T_c such an extra spin wave contribution to the susceptibility is proportional to the square of the tunneling frequency for reorientation of the NO_2^- group. This frequency may be quite low, at least by comparison with the tunneling frequency in hydrogen-bonded ferroelectrics. The sensitivity of reflectivity measurements is not well suited to the detection of very small changes in the dielectric response.

If additional confirmation is needed for the conclusion that none of the infrared modes studied here is responsible for the dielectric anomaly near the ferroelectric Curie point, it is only necessary to repeat the dispersion measurements at higher temperatures. We have, in fact, redetermined the b-axis reflectance of $NaNO_2$ near 170°C, finding generally good agreement with Vogt and Happ,[9] who made more extensive measurements at several temperatures up to 200°C. These measurements clearly reveal both shifting and broadening of the dispersion frequencies beyond what might be termed normal temperature effects and must almost certainly be connected with the loss of long-range order in the lattice. However, it is equally certain that the changes in observed mode frequencies and strengths can account at best for only a small part of the behavior of the low-frequency dielectric response near T_c.

In summary, the present study of the infrared dielectric response of $NaNO_2$ has attempted to establish the following points:

(1) A rather complete experimental determination of the infrared spectral reflectance and, by use of Kramers-Kronig relations, the lattice dielectric response function.

(2) The dispersion frequencies identifiable from the dielectric response are explainable as frequencies associated with normal polar vibrational modes of the ordered $NaNO_2$ lattice. In particular, it is established that there is no sizeable resonant infrared contribution to the dielectric response which can be attributed to either a soft phonon mode or to an additional spin-wave-like mode of excitation involving positional disordering of the NO_2^- group. The failure to observe a mode of the latter type, the existence of which seems fundamental to a proper dynamical theory of order-disorder transitions, is probably the result of excessive damping and small dipole strength well below the ordering temperature.

(3) The dipole strengths of the polar vibrational modes are discussed by introducing the concept of apparent ionic charges. The electronic polarization effects greatly modify the static ionic charges to produce anisotropic apparent charge tensors. These effects are calculated in detail for $NaNO_2$ in the dipole field approximation, and it is found that this treatment can account quite well for the observed dipole strengths. Details of the charge distribution within a unit cell can be directly inferred. The most reliable such deduction is that the static charge associated with the Na ion is very close to unity.

ACKNOWLEDGMENTS

The excellent samples of $NaNO_2$ were grown by J. E. Scardefield by a method developed by him. The reflectance measurements were capably performed by R. Hammer and G. D. Pettit. The computer program for calculating the dipole sums was generously provided by Dr. G. E. Schacher and D. B. Dickmann. The author appreciatively acknowledges these contributions.

[29] D. Hadzi, J. Chem. Phys. **34**, 1445 (1961).
[30] A. S. Barker, Jr., and M. Tinkham, J. Chem. Phys. **38**, 2257 (1963).